Measurements of the Threshold Displacement Energy in Ta and Nb†

G. YOUNGBLOOD, S. MYHRA, AND J. W. DEFORD
Department of Physics, University of Utah, Salt Lake City, Utah 84112
(Received 19 May 1969)

Changes in the damage rate (residual electrical resistivity per unit electron fluence) were measured as a function of incident electron energy in the range 1.0–2.2 MeV for 0.002-in.-diam Nb and Ta wires. The threshold energies, estimated by simple extrapolation to zero production rates, were 36 eV for Nb and 32 eV for Ta. The resistivity of a Frenkel pair was determined to be about 5.3 $\mu\Omega$ cm/at.% for Nb and 1.9 $\mu\Omega$ cm/at.% for Ta. The damage production curves for two other bcc metals, Mo and W, are compared with those for Nb and Ta.

I. INTRODUCTION

THIS experiment was performed in two parts. The first part is described in Paper I[1] and deals with the concentration dependence of the defect annealing spectrum after electron irradiation of Nb and Ta. Hereafter, Paper I and experiment will be designated by I. In this paper, we report measurements of the rate of defect production in Nb and Ta irradiated below 24°K with electrons in the energy range 1.0–2.2 MeV. In particular, the threshold energy for lattice displacement T_0 and the resistivity per unit Frenkel defect concentration ρ_F are determined. Past work has indicated that the threshold-energy surface is highly anisotropic in the bcc metals.[2,3] We have tried to fit the experimental damage rate data with a theoretical damage rate prediction, using a simple-step function for $\rho_d(T)$, the probability of displacement function.[4] This model contains two adjustable parameters ρ_F and T_e, where T_e is the effective threshold energy for lattice displacement. A T_e different than T_0 is a rough measure of the importance of directional effects; $T_e \approx T_0$ indicates that the threshold energy surface is essentially isotropic.

A brief description of the experimental equipment and techniques is given in Sec. II. The experimental results are discussed in Sec. III. These results are compared to those obtained from similar experiments on Mo [5] and W.[6]

II. EXPERIMENTAL

This experiment was performed as the complement of the experiment in I. Thus the helium cryostat, sample preparation and mounting, and the resistance and temperature monitoring system are fully described there. Only the modifications necessary to convert an annealing experiment into a damage production experiment will be described here.

The samples irradiated were a single pair of the six Nb and Ta samples described in I. The resistance ratios are listed in Table I of Paper I. Resistance ratio measurements made after the annealing experiment and prior to this experiment indicate that about 20% of the damage remained after warming to room temperature.

The flux distribution in the beam was not homogeneous. The distribution was determined as follows. The beam profile was adjusted to a particular radial distribution by means of a quadrupole magnet system. A beam-distribution measuring device consisting of four insulated brass disks with successively smaller holes mounted in the charge collector was used to monitor the beam profile continuously. Once the radial profile was determined, an average flux could be estimated by integrating over the length of the active part of the sample. It was decided to use a flux pattern which dropped off by about one-third at each end of the sample. With the focusing magnets set to provide this, the beam itself could be used as a probe to check alignments. Calibration of the beam energy was performed prior to the experiment using the standard Be (γ,n) threshold reaction at 1.665 MeV. There were no intervening foils between the accelerator and the samples.

Both Ta and Nb have low-thermal conductivities at 20°K; therefore, the measuring current was limited to 20 mA in order to maintain an acceptable temperature gradient (0.1°K/cm) along the samples.

Reasonable voltage changes (about 1.0 μV per irradiation period) required irradiation periods from 3 h at 2.2 MeV to 20 h at 1.0 MeV. All resistance measurements were made at a reference temperature of 19.50 $\pm$0.25°K. (Ta and Nb are superconducting; therefore, a temperature above that of liquid helium was used for a reference.) The effects of small temperature fluctuations and transients were eliminated by using a dummy sample calibrated against a platinum resistance thermometer.[1]

Since the damage production measurements for the concentration-dependence experiment described in I have some bearing on the interpretation of this experiment, these measurements will now be described.

† Research supported by the U. S. Atomic Energy Commission, under Contract No. AT (11-1)1494.

[1] S. Myhra and J. W. DeFord, preceding paper, Phys. Rev. **185**, 1093 (1969).
[2] C. Erginsoy, G. H. Vineyard and A. Englert, Phys. Rev. **133**, A595 (1964).
[3] H. H. Andersen and P. Sigmund, Risö Report No. 103, 1965 (unpublished).
[4] A. Sosin, Phys. Rev. **126**, 5 (1962).
[5] P. G. Lucasson and R. M. Walker, Phys. Rev. **127**, 485 (1962).
[6] H. H. Neely, D. W. Keefer, and A. Sosin, Phys. Status Solidi **28**, 675 (1968).

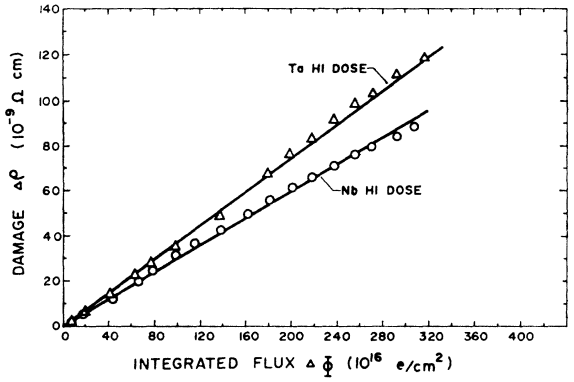

FIG. 1. Damage rate for high-dose Nb and Ta. These are the damage production curves for the samples used in the concentration-dependence experiment (Ref. 1). Temperature during irradiation, 15°K. No corrections are applied.

Figure 1 shows the damage production at 2.2 MeV for the high-dose Nb and Ta samples; the temperature during irradiation was 15°K. There was no noticeable annealing in the high-dose samples during a period of 20 h when the electron beam was shifted to the medium- and low-dose samples. The damage production curves are linear within experimental error to a fluence of about 3×10^{18} electrons/cm^2.

During the threshold energy experiment measurements of the resistance changes were made after three different intervals of irradiation for each energy.

The sample heating was monitored during irradiation and a temperature rise of less than 6.0°K was maintained. This placed an upper limit on the beam current density—nominally 1.7 μA/cm^2. Sample temperatures during bombardment actually ranged 24.8–25.7°K in Nb and 22.4–23.4°K in Ta.

III. EXPERIMENTAL RESULTS

It is pointed out above that the damage rate curves for the concentration-dependence experiment showed linearity to the highest fluences. Since the total damage induced during the threshold energy experiment was

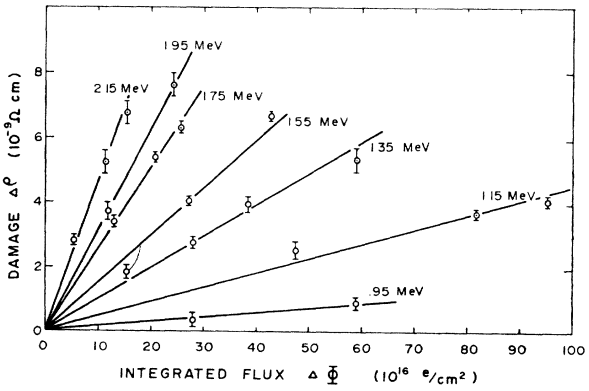

FIG. 2. Damage rate in Nb. Corrections applied: energy degradation and simultaneous annealing. The temperature during irradiation was ~25°K.

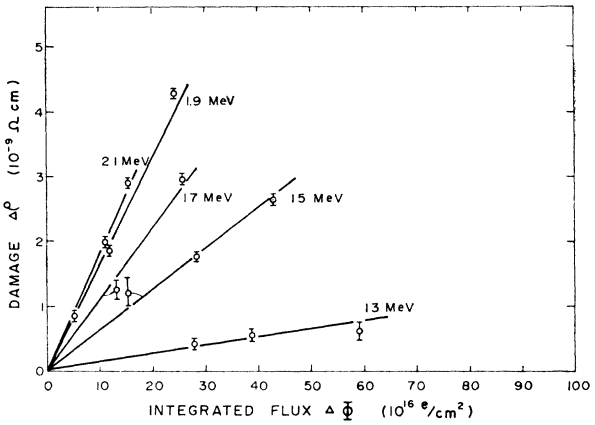

FIG. 3. Damage rate in Ta. Corrections applied: energy degradation and simultaneous annealing. Temperature during irradiation, ~23°K.

less than that induced during the experiment of I, we assume that the damage production here is also linear. Figures 2 and 3 show the experimental damage rate with energy degradation and simultaneous annealing corrections applied for each electron bombarding energy.

The integrated flux measurements have a random error which was estimated to be less than $\pm2\%$. The beam pattern, however, was not homogeneous across the entire sample—so there does exist some uncertainty as to what to use for "the fluence." Since residual resistance measurements are an average measure of defect concentration along the length of the active sample, the change in residual resistance corresponds to an average fluence along the length of the sample.

The deviations from linearity in the damage rate curves of Figs. 2 and 3 are then assigned to errors in the resistance measurements. The "adjustment" to the reference temperature of 19.50°K, necessary in a few cases, required corrections up to ±0.50 μV for the potentiometer readings. The error bars on the resistance measurements reflect the uncertainty associated with this large correction. Thus $\Delta\rho/\Delta\Phi$ was calculated from

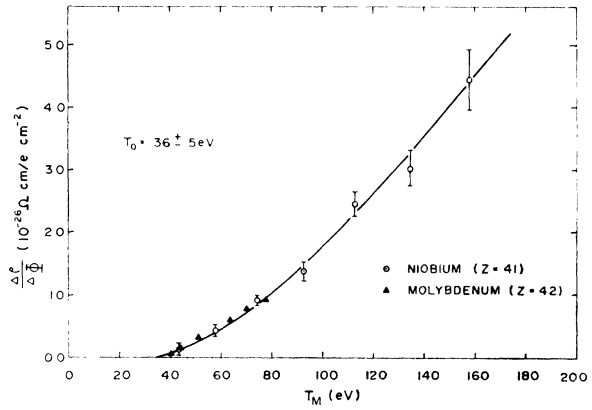

FIG. 4. Damage production for Nb and Mo as a function of T_M. Corrections applied: energy degradation, electron straggling, and simultaneous annealing.

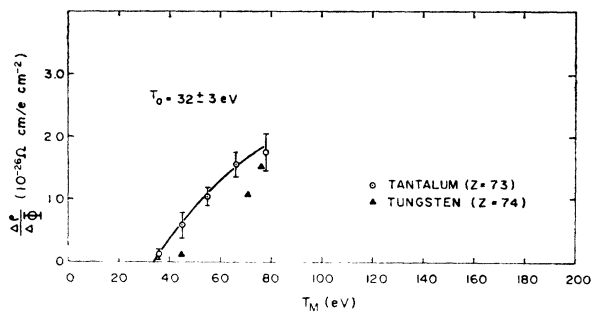

FIG. 5. Damage production for Ta and W as a function of T_M. Corrections applied: energy degradation, electron straggling, and simultaneous annealing. There are no corrections applied for W.

the best-fit straight line to the corrected data of Figs. 2 and 3, where the fit was obtained by minimizing the vertical deviations (deviations in $\Delta\rho$).

Figures 4 and 5 show the final results of the resistivity increase per unit electron fluence, $\Delta\rho/\Delta\Phi$, as a function of T_M for Nb and Ta, respectively. T_M is the maximum kinetic energy transferred to a nucleus after a head-on collision by a bombarding electron. These results are corrected for energy degradation of the electron beam, multiple scattering, and some slight simultaneous annealing during the irradiation. No corrections are made for the sample receiving only partial damage near the front portion when the electron energy is near threshold, nor for the electron beam having a slight distribution in energy. The measurements reported here extend well above threshold and should not be affected in that region. However, extrapolation of the damage rate curves through the near-threshold region are performed with the reservation that a detailed analysis would require these corrections also.

The first correction yields an estimate of the average energy of an electron at the midpoint of the wire sample, $\bar{E}$; T_M was then calculated using the formula $T_M = 560.8 \times (x+2)/A$, where A is the atomic weight, and x is $\bar{E}/m_0c^2$.[7] The multiple-scattering correction accounts for the increased path length of the electron within the sample which can be thought of as an increase in the effective flux. We modified Sosin's[4] method of correcting for electron straggling in a thin foil to apply to our thin wire samples. We obtained an "equivalent foil thickness" by setting $\pi r^2 = t^2$, where r is the sample radius and t is the equivalent thickness.

It has been reported by Hemmerich *et al.*[8] and by Burger *et al.*[9] that annealing occurs at 9 and 15°K and in Paper I as 23°K for Ta. Likewise, Burger shows an annealing peak at 15°K and I shows a peak at 26.5°K for Nb. In all of these studies it is emphasized how the presence of impurities in the range of a few hundred ppm almost completely suppressed the low-temperature annealing substages. Paper I also proposes that a two-interstitial model seems to fit the annealing characteristics best where stage I (the 9 and 15°K peak in Ta and the 15°K peak in Nb) was assigned to the free migration of a type-A interstitial defect and stage II (20–120°K in Ta and 20–50°K in Nb) was assigned to the release from traps and the subsequent annihilation of the type-A interstitial. If the concentration of impurities is much larger than the vacancy concentration, the impurities tend to trap the freely migrating interstitial defect responsible for stage-I annealing before it can annihilate at a vacancy. In this way no appreciable damage is lost until stage-II temperatures are reached, i.e., where interstitial release from traps begins to occur. For instance, no annealing took place in either the Ta or Nb high-dose samples while the medium-dose samples were being irradiated even though the temperature was near 15°K. The high impurity concentration has suppressed the annealing due to the 15°K free-migration peak. However, the temperature during irradiation in the threshold experiment reaches the temperature range assigned to stage II (greater than 20°K). Thus, some annealing occurs simultaneously with the damage production and this annealing follows first-order kinetics. In order to obtain helium-temperature damage rates, a small correction factor to account for the simultaneous annealing can be applied. The estimation of a correction factor for annealing is developed in the Appendix.

Lucasson and Walker[5] performed damage production measurements on Mn using liquid hydrogen as a refrigerant. Their Mo sample had a comparable impurity content to our samples. They stated that the damage production rate in Mo was enhanced by about 10% when they repeated the experiment using liquid helium as refrigerant. This compares favorably with the 6% simultaneous annealing correction we obtained for Nb.

Table I summarizes the magnitude of the corrections applied to the damage rate curves. The electron-straggling and simultaneous-annealing corrections are relatively lower for the higher bombardment energies and gradually increase as the threshold energy is approached. The impurity content of both Nb and Ta was high enough so that surface scattering corrections to the bulk resistivity could be ignored.

TABLE I. Corrections to damage rate curves.

Correction	Ta	Nb
Energy degradation	−0.10 MeV	−0.05 MeV
$\Delta\Phi(E)$, electron straggling	+4–10%	+3–12%
$\Delta\rho(E)$, simultaneous annealing	+5–10%	+6%

[7] J. W. Corbett, *Electron Radiation Damage in Semiconductors and Metals* (Academic Press Inc., New York, 1966).

[8] H. Hemmerich, D. Meissner, H. Schultz, and F. Walz, in Proceedings of the Conference on Interstitials and Vacancies, Jülich, Germany, 1968 (unpublished).

[9] G. Burger, K. Isebeck, R. Kerler, J. Völkl, H. Wenzel, H. R. Kuhlmann, and H. Schultz, Phys. Letters **20**, 470 (1966).

Figure 4 also shows the damage production curve for Mo as measured by Lucasson and Walker,[5] and Fig. 5 shows three preliminary measurements for W by Neely *et al.*[6] For all four meals the threshold energy is approximated by simple extrapolation of the damage production curve to zero rate of production; the intercept of the T_M axis yields the threshold displacement energy T_0. The samples are polycrystalline; therefore, T_0 is the minimum energy required to displace an atom in the "easiest" crystalline direction.

To analyze the data further, we assume that ρ_F, the specific resistivity per unit concentration of Frenkel defects, represents the combined effects of a well-separated interstitial-vacancy pair even though the interstitial may be trapped or exist in various configurations. Theory and experiment are compared through the relation

$$(\Delta\rho/\Delta\Phi)_{\text{expt}}=\rho_F(\sigma_d)_{\text{theor}}. \tag{1}$$

The cross section for atomic displacement, σ_d, was determined from

$$\sigma_d=\int_0^{T_M} P_d(T)\frac{d\sigma}{dT}(T,T_M)dT, \tag{2}$$

where $d\sigma(T,T_M)$ is the differential cross section for transfer of energy T from an electron capable of transferring at most an energy T_M to a nucleus. $P_d(T)$ is the probability of a nucleus, endowed with a recoil energy T, actually being displaced. The step-function displacement model has been used for the primary displacements; secondary displacements are accounted for by the Kinchin and Pease[10] cascade model with no energy loss to the lattice during primary displacements. Thus, we have

$$\begin{aligned} P_d(T)&=0, && 0<T<T_e\\ &=1, && T_2\leq T<2T_e\\ &=T/2T_e, && 2T_e\leq T\leq T_M. \end{aligned} \tag{3}$$

Using the displacement model of Eqs. (3) and the relationship for $T_M(E)$ to rewrite Eq. (2) more explicitly, Oen[11] gets the following expressons for the total-displacement cross section:

$$\sigma_d(E)=\frac{0.06515Z^2(E+0.511)^2}{E^2(E+1.022)^2}\int_{x_e}^1\frac{dx}{x^2}M(x,E) \tag{4}$$

in barns for $0.5\leq x_e\leq 1$, and

$$\sigma_d(E)=\frac{0.06515Z^2(E+0.511)^2}{E^2(E+1.022)^2}\times\left(\int_{x_e}^{2x_e}\frac{dx}{x^2}M(x,E)+\int_{2x_e}^1\frac{1}{2x_e}\frac{dx}{x}M(x,E)\right), \tag{5}$$

in barns for $x_e<0.5$, where $x=T/T_M$, $x_e=T_e/T_M$, $Z=$the atomic number, $E=$the average electron energy at the sample midpoint, and $M(x,E)$ is the ratio of the Mott cross section to the Rutherford cross section. If we have $M(x,E)=1$ over the entire interval of integration, Eqs. (4) and (5) are precisely the classical Darwin-Rutherford displacement cross sections.

The ratio $M(x,E)$ was taken from data for Mo and W published by Oen,[11] who evaluated this ratio using the numerical method of Doggett and Spencer.[12] This ratio is slowly varying with Z; thus linear interpolation was used to obtain the ratios for Nb and Ta. The integrals were computed numerically using small successive intervals of integration of 0.05. This approximation to the Mott cross section is accurate within 2%; the inaccuracy is primarily due to the method of performing the integration. The displacement model itself warrants no better accuracy than this.

Theory and experiment are forced to agree by adjusting the parameters ρ_F and T_e to obtain the best fit of $(\Delta\rho/\Delta\Phi)_{\text{expt}}$ versus $\rho_F(\sigma_d)_{\text{theor}}$ over as much of the energy range as possible and favoring the lower portion of the energy range. In this way we estimated ρ_F from Eq. (1) by using $(\Delta\rho/\Delta\Phi)_{\text{expt}}$ and $\sigma_d(E)$ from Eq. (4), both evaluated at $T\approx 2T_0$. In effect, this represents the best normalizing point for cross-section calculations because $P_d(T)$ should be close to unity at this energy for the following reasons. First, this energy is just below the point where multiple displacements can occur according to the Kinchin-Pease model; and, second, even if the recoil angle is large, the energy transferred to the nucleus is still sufficient for a displacement. Also, the experimental data have better precision and the corrections are of smaller magnitude at this point.

Figure 6 shows how ρ_F and T_e are adjusted to force $\Delta\sigma/\Delta\Phi$ to agree with theory at the normalizing energy of 1.9 MeV for Ta. The curve for $T_e=32$ eV and $\rho_F=1.9$ $\mu\Omega$ cm/at.% agrees well for the three experimental points of electron energy lower than 1.9 MeV. Figure 7 shows the same data replotted except that all the theoretical curves are calculated for a fixed $\rho_F=1.9$ $\mu\Omega$ cm/at.% and various T_e.

Figures 8 and 9 show a similar set of curves for Nb. The normalizing energy was 1.35 MeV. The curves for $T_e=40$ eV and $\rho_F=5.3$ $\mu\Omega$ cm/at.% fits the experimental data best at the lower bombardment energies. However, there is a sharp change in slope of the damage rate curve near 1.6 MeV; the experimental points for energies higher than this do not fit a simple step-function probability of displacement model. For instance, in an effort to preserve the simple step function, a higher ρ_F was introduced in order to fit the high-energy data. Figure 8 shows a dashed curve for $\rho_F=10$ $\mu\Omega$ cm/at.% and $T_e=44$ eV. This, of course, will not yield the sharp break in the damage rate curve. The most

[10] G. H. Kinchin and R. S. Pease, Repts. Progr. Phys. 18, 1 (1955).

[11] O. S. Oen, Oak Ridge National Laboratory Report No. ORNL-3813, 1965 (unpublished).

[12] J. A. Doggett and L. V. Spencer, Phys. Rev. 103, 1597 (1956).

plausible explanation for the break is that the single-step displacement model does not apply to Nb. The threshold energy surface must be highly anisotropic with a

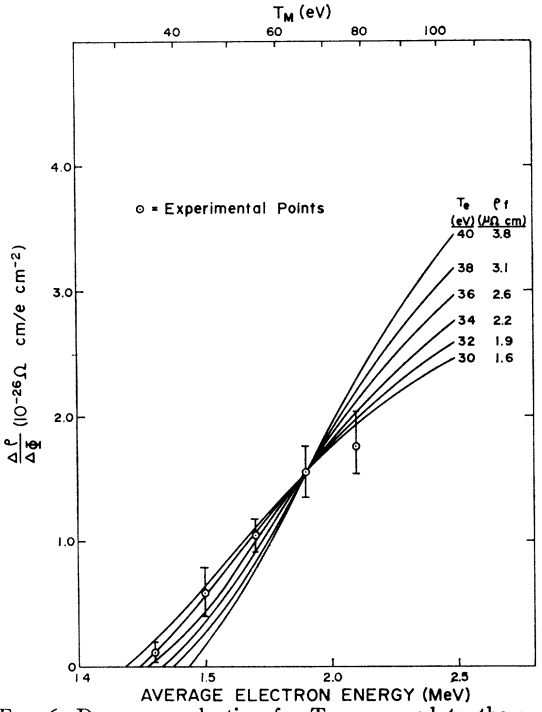

FIG. 6. Damage production for Ta compared to theory by adjusting the parameters T_e and ρ_F. $\Delta\rho/\Delta\Phi$ is normalized at 1.90 MeV.

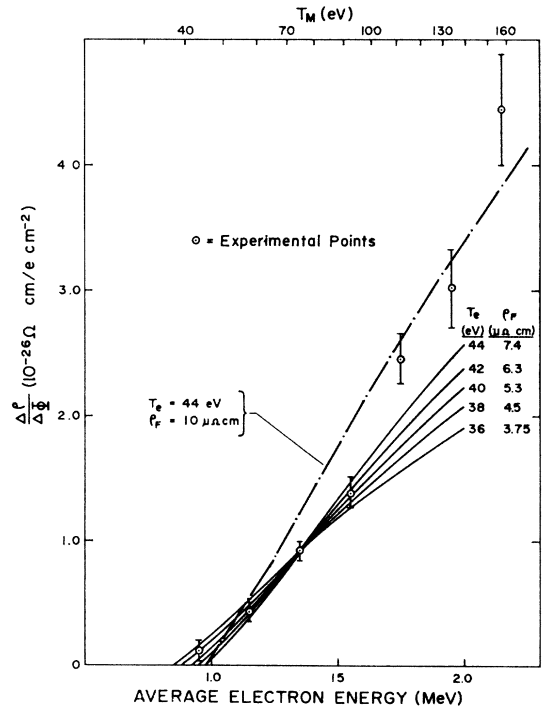

FIG. 7. Damage production for Ta compared to theory for various values of T_e. $\rho_F = 1.9$ μΩ cm/at.%.

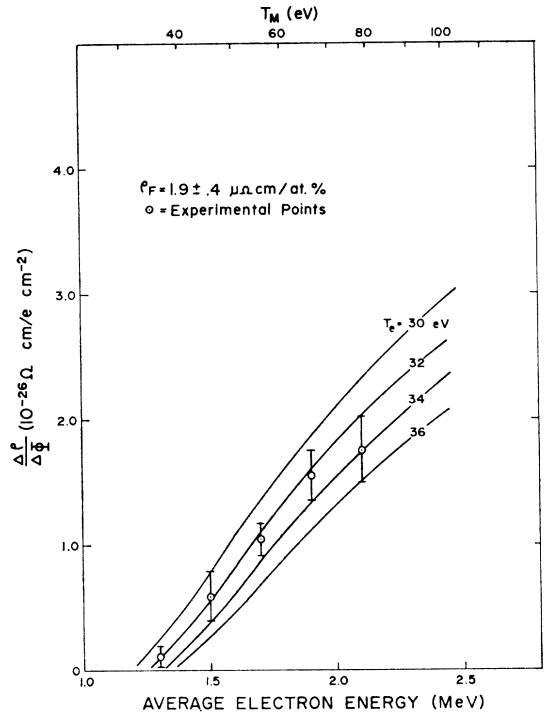

FIG. 8. Damage production for Nb compared to theory by adjusting the parameters T_e and ρ_F. $\Delta\rho/\Delta\Phi$ is normalized at 1.35 MeV.

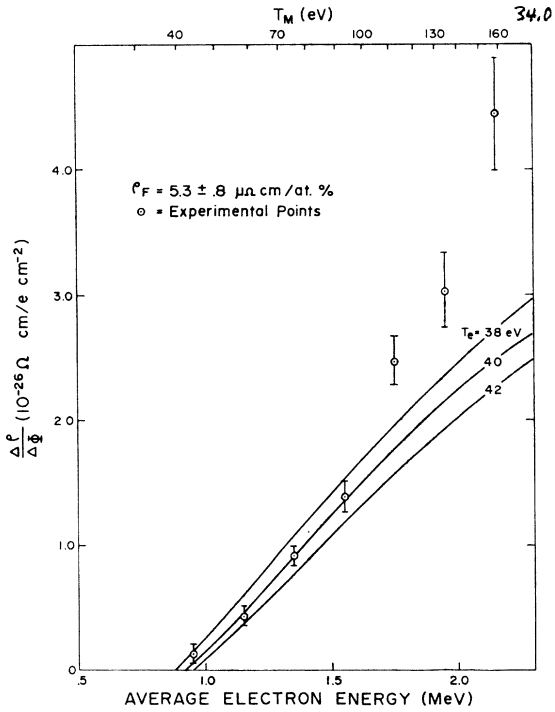

FIG. 9. Damage production for Nb compared to theory for various values of T_e. $\rho_F = 5.3$ μΩ cm/at.%.

secondary threshold minima near 90 eV. If this is the case, ρ_F would be greater than the stated 5.3 μΩ cm/at.% also.

Lucasson and Walker[5] were the first to propose that the threshold energy surface for bcc metals is highly anisotropic when they found that a "two-step staircase displacement probability function" allowed them to fit their damage rate data for iron the best. They used the following $P_d(T)$:

$$P_d(T)=0.0, \quad T<22 \text{ eV}$$
$$P_d(T)=0.6, \quad 22 \text{ eV} \leq 66 \text{ eV}$$
$$P_d(T)=1.0, \quad T>66 \text{ eV}.$$

Later, computer simulation of the damage process in Fe by Erginsoy *et al.*[2] resulted in a mapping of the threshold energy contours over the fundamental stereographic triangle. By numerical integration, the displacement probability function obtained was

$$P_d(T)=0.0, \quad T<17 \text{ eV}$$
$$P_d(T)\approx 0.25, \quad 17 \text{ eV}<T<38 \text{ eV}$$
$$P_d(T)\approx 0.75, \quad 38 \text{ eV}<T<T_M.$$

They also obtained $T_D\langle 100\rangle=17$ eV and $T_d\langle 111\rangle=38$ eV.

Andersen and Sigmund[3] have made the most extensive theoretical predictions of the threshold energy for the low-index directions for both fcc and bcc metals. They considered the repulsive interaction between two atoms in a crystal to be represented by a Born-Mayer potential $V(r)=Ae^{-r/a}$, and two types of collision sequences to be accounted for the energy loss to the lattice by the primary struck nucleus. They used the experimental threshold energies $T_d\langle 110\rangle \approx T_d\langle 100\rangle \approx 19$ eV for Cu single crystals measured by Sosin and Garr[13] to determine that $a=0.18$–0.23 Å and $A=41$–6.1 keV for Cu. They then generalized the Born-Mayer potential by adopting $a=0.219$ Å for all elements and $A=52Z^{3/2}$ keV, a function of atomic number only. Making estimates about the dominant energy-loss mechanism for various directions in fcc and bcc metals, Andersen and Sigmund worked backwards from their generalized Born-Mayer potential to predict the threshold energies for the other metals. With the exception of Al their predictions agree well with experimental values of T_d for the fcc metals. Their predictions for bcc metals are generally lower in value than the available experimental results. The dominant feature of their predictions is that $T_d\langle 110\rangle \approx T_d\langle 100\rangle$ for fcc metals and that $T_d\langle 111\rangle \approx 2.4T_d\langle 100\rangle$ for bcc metals.

If one assumes that the two minima in fcc metals are rather broad, then T_0 will be approximately equal to $T_d\langle 110\rangle$ and $T_d\langle 100\rangle$ and also to T_e. The threshold energy surface is fairly isotropic and the single-step function $P_d(T)$ should describe the damage production in a fcc polycrystal as is the case for Cu, Al, Pt, Pa, Au, Ni, and Ag.[7]

[13] A. Sosin and K. Garr, Phys. Status Solidi 8, 481 (1965).

TABLE II. Summary of threshold energies and specific resistivities for Nb, Mo, Ta, W, and Fe.

Z	41	42	73	74	26
Experimental					
T_0 (eV)	36±5	34	32±3	40±2	16
T_e (eV)	40(90)	37	32		22(66)
ρ_F($\mu\Omega$ cm/at.%)	>5.3	>4.5	>1.9	>2.7[a]	19
Theoretical[b]					
$T_d\langle 100\rangle$ (eV)	11	15	25	34	14
$T_d\langle 111\rangle$ (eV)	26	35	61	80	31

[a] Estimated from the author's published damage rate of 1.08×10^{-26} $\mu\Omega$ cm/e cm^{-2} and from Oen's (Ref. 11) calculation of $\sigma_d=40\times10^{-24}$ cm^2 at $\bar{E}=1.9$ MeV and assuming a T_e of 40 eV.
[b] From Ref. 3.

The situation is different for the bcc metals where the local threshold minima are about the $\langle 100\rangle$ and the $\langle 111\rangle$ directions and are apparently quite different. Damage along the $\langle 110\rangle$ direction is restricted by the high potential barrier of only two atoms so that the straight-line orbit along $\langle 110\rangle$ is not stable according to Andersen and Sigmund.[3] Table II lists the threshold energy predictions of Andersen and Sigmund for five bcc metals along with the experimental observations of others for Mo, Fe, and W, and of this experiment for Nb and Ta. Only for Nb and Fe has the electron bombarding energy been carried high enough ($T_M>3T_0$) to show explicitly the two-step nature of $P_d(T)$. The ratio $T_d\langle 111\rangle/T_d\langle 100\rangle \approx 2.4$ from the theoretical predictions listed in Table II compares well with the ratio of the two-step T_e, 2.2_5 for Nb and 3.0 for Fe, which are determined by fitting experimental damage rates to theory. The secondary minima are enclosed in parentheses in Table II.

We have not tried to fit our experimental damage rates with a two-step $P_d(T)$, but the data indicate that this type of probability function should be used for bcc metals, in general. The calculated ρ_F values thus should exceed the listed values in Table II as is indicated by the > sign.

IV. SUMMARY

The threshold energy for atomic displacements in Nb was found to be 36±5 eV and in Ta was found to be 32±3 eV.

The damage rate curves for bcc metals are similar. The $P_d(T)$ function should be two step in nature with the second step occurring at $\approx 2.4T_0$, corresponding to a highly anisotropic threshold energy surface.

The change in electrical resistivity per at.% concentration of Frenkel defects ρ_F should be greater than 5.3 $\mu\Omega$ cm for Nb and 1.9 $\mu\Omega$ cm for Ta.

ACKNOWLEDGMENTS

The authors wish to thank Dr. Abraham Sosin for his careful reading of this paper and Dr. Peter Sigmund for his critical analysis of the results.

APPENDIX

The following are the simultaneous-annealing correction assumptions:

(1) The specific resistivity of a Frenkel defect ρ_F is a constant independent of defect configuration or trapping.

(2) $\Delta\rho/\Delta\Phi=\rho_F\sigma_d=\rho\sum_{Fi}\sigma_d{}^i$. Each defect configuration has its own cross section for displacement and has the same threshold energy. This means that the distribution of types of defects is independent of the bombarding energy.

(3) The annealing follows first-order kinetics as is assigned to stage II.[1]

Consider only the production of a single type of defect characterized by an annealing rate coefficient $K_1=\nu_0 e^{-e/kT}$ and a production rate $R_1(E)$ proportional to $\rho_F\sigma_d{}^1(E)$, where $\sigma_d{}^1(E)$=displacement cross section for the defect under consideration, ν_0=frequency factor, e=activation energy for migration of interstitial, k=Boltzmann's constant, T=absolute temperatrue, and E=electron bombardment energy. The differential equation that describes the competing processes of production and annihilation of defects as a function of time is then

$$d\Delta V_1/dt=R_1(E)-K_1\Delta V_1, \tag{A1}$$

where ΔV_1 is the measured voltage change. We solved the differential equation in terms of voltage, which is directly proportional to the resistivity change. If ΔV_0 is the voltage accumulation at the start of each measuring interval, Eq. (1) has the solution

$$\Delta V_1=(R_1/K_1)(1-e^{-K_1t})+\Delta V_0 e^{-K_1t}. \tag{A2}$$

We evaluated K_1t for each measuring interval with $\nu_0=5\times10^{11}$ sec^{-1}, $E_{act}=0.075$ eV (the activation energy of the lowest stage-II annealing peak in Nb taken from I), T=the average sample temperature during irradiation for each bombarding energy, and t=the irradiation time for each measuring interval. K_1t ranged 215–10 for all intervals. Thus, to a good approximation, we have

$$\Delta V_1\rightarrow R_1/K_1.$$

The production of this defect reaches a steady-state condition after which essentially no accumulation of this type of defect occurs. Ten percent of the damage annealed out in the annealing experiment[1] below the temperature at which these samples were bombarded. Therefore we take $R_1=0.1R_{He}$, where R_{He} is the intrinsic production rate when no annealing is going on simultaneously during production. Now the measured voltage change can be corrected for each interval, since

$$\begin{aligned}\Delta V_{meas}&=\Delta V_{rest}+\Delta V_1-\Delta V_0\\&=0.9R_{He}t+\frac{0.1R_{He}t}{K_1t}(1-e^{-K_1t}\\&\qquad+\Delta V_0 e^{(-K_1t)-1}\\&=\Delta V_{He}[0.9+(0.1/K_1t)(1-e^{-K_1t})]\\&\qquad+\Delta V_0(e^{-K_1t}-1).\end{aligned} \tag{A3}$$

ΔV_{He}, the voltage change for each measuring interval without simultaneous annealing, is then found from Eq. (3):

$$\Delta V_{He}=\frac{\Delta V_{meas}+\Delta V_0(1-e^{-K_1t})}{0.9+(0.1/K_1t)(1-e^{K_1t})}. \tag{A4}$$

The high-temperature limit of Eq. (4) is obtained by letting K_1t be large and ΔV_0 small. The simultaneous-annealing correction applied in our experiment corresponded to about this limit.

The correction was 5–10%; thus the rather crude approximations made are justified by the smallness of the correction factor.